arXiv:1407.7287v2 [physics.atom-ph] 3 Oct 2014

Optimization and error model for atom interferometry technique to measure Newtonian gravitational constant

B. Dubetsky
bdubetsky@gmail.com
(Dated: October 6, 2014)

Considered contribution to the phase of the atom interferometer caused by the gravity field of the massive proof mass. Demonstrated the method of finding the extrema of this contribution for 100kg Tungsten proof mass of the specific shape and specific parameters of ^{133}Cs atom interferometers. Calculated variations of the double difference response under the small deviations of atomic and proof mass variables. The choice of the extremal values of the atomic variables allows one to release requirements for atom positioning on 2 orders of magnitude.

Atom interference [1] is one of the tool to measure Newtonian gravitational constant [2, 3]. An atomic gravity-gradiometer [4] is used in this measurements. When one initially launches the atom cloud at position $\vec{a}$ with velocity $\vec{v}$ on the one of the hyperfine sublevel F_g of the atomic ground state manifold and applies at the moments

$$\tau = \{t_1, t_1 + T, t_1 + 2T\} \tag{1}$$

$\frac{\pi}{2} - \pi - \frac{\pi}{2}$ sequence of the Raman pulses resonant to the atomic transition to another hyperfine sublevel F_e, the population of the sublevel F_e, after interaction, contains [5] interferometric term, whose phase is linear on the gravity field $\vec{g}(\vec{x})$. In Eq. (1) t_1 is time delay between moments of atom launching and first Raman pulse and T is time separation between pulses. Measuring, in the Earth gravity field $\vec{g}_E(\vec{x})$, the phase difference $\Delta\phi$ between two interferometers with clouds launched at positions and velocities $\{\vec{a}_1, \vec{v}_1\}$ and $\{\vec{a}_2, \vec{v}_2\}$, one gets signal linear on the Earth gravity field gradient tensor [4]. When this gravity-gradiometer operates in the presence of the proof mass W, the total gravity field

$$\vec{g}(\vec{x}) = \vec{g}_E(\vec{x}) + \delta\vec{g}(\vec{x}), \tag{2}$$

where $\delta\vec{g}(\vec{x})$ is proof mass gravity field, and therefore the atom interferometer's phase is linear on $\delta\vec{g}(\vec{x})$. Performing these measurements for two positions of the proof mass, which we call below "joined" and "separated" and calculating the difference of the measurements, one gets the double difference of phases, $\delta\Delta\phi$, which is evidently caused only by the proof mass field $\delta\vec{g}(\vec{x})$. This double difference of phase we call response

In this article we determine numerically optimal positions and velocities $\{\vec{a}_i, \vec{v}_i\}$ to maximize the response and determine the sensitivity of the response to the variations of the atomic and proof mass variables. For the part of the atom interferometer phase, caused by the proof mass, which we call below just "phase", one can use expression [6]

$$\phi = \vec{k} \cdot (\tau_3 \vec{u}_{30} - t_1 \vec{u}_{20} + \vec{u}_{21} - \vec{u}_{31}), \tag{3a}$$

$$\vec{u}_{\alpha\beta} = \int_{\tau_{\alpha-1}}^{\tau_\alpha} dt t^\beta \delta\vec{g}\left(\vec{a} + \vec{v}t + \vec{g}_E\frac{t^2}{2}\right), \tag{3b}$$

where $\vec{k}$ is effective Raman wave vector, τ_i is defined in Eq. (1). Expression (3) was derived under assumptions

1. proof mass gravity field has small magnitude ($|\delta\vec{g}(\vec{x})| \ll |\vec{g}_E|$) but arbitrary inhomogeneity;
2. recoil effect is negligible;
3. Earth gravity field is permanent $\vec{g}_E(\vec{x}) \equiv \vec{g}_E$
4. clouds' temperature is sufficiently small to neglect Raman resonance Doppler broadening during pulse duration and clouds' thermal expansion during time $t_1 + 2T$;
5. clouds' size is sufficiently small to neglect ac-Stark shift variation and wave front curvature along the clouds.

I. OPTIMIZATION

Even though Eq. (3) can be applied for any proof masses, including those chosen in [2, 3], we present here results of former calculations performed for specific case shown in Fig 1

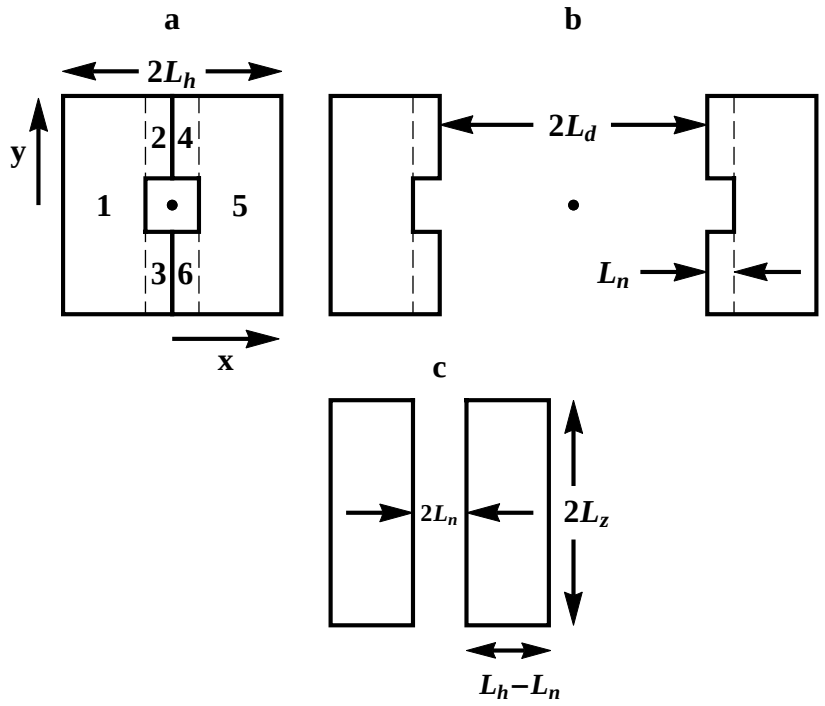

FIG. 1: The proof mass as a whole is parallelepiped $2L_h \times 2L_h \times 2L_z$ with narrow $2L_n \times 2L_n \times 2L_z$ hole for Raman fields and atom trajectories. Atoms are launched vertically from the points z_1 and z_2 with velocities v_{1z} and v_{2z}. Proof mass consists from 2 halves. (a) Top view. Joined halves. (b) Top view. Halves separated on the distance $2L_d$ along x access. (c) Side view, cross-section $x = 0$.

Scale of the parameters chosen for calculations are pieced together in the Table I. The chosen value of density corresponds to pure Tungsten [7].

For the given proof mass difference between phases of the interferometers $\{z_1, v_{1z}\}$ and $\{z_2, v_{2z}\}$ is maximal when $\{z_1, v_{1z}\}$ is an absolute maximum of the phase and $\{z_2, v_{2z}\}$ is an absolute minimum of the phase. To find out these extrema we used an iterative process, which was continued until the new value of the extremum differs relatively from the previous value less than measurement accuracy

$$err = 10^{-4}. \tag{4}$$

Our choice of the proof mass shape is convenient because for the gravity potential of the parallelepiped having

TABLE I: Order of magnitude of the atom interferometer and proof mass parameters

Atom	^{133}Cs
Effective wave vector	$\vec{k} = \{0, 0, k\}\,,\ k = 1.47 * 10^7 \mathrm{m}^{-1}$
Time between launch and first Raman pulse	$t_1 \sim 40\mathrm{ms}$
Time between Raman pulses	$T \sim 250\mathrm{ms}$
Relative acuracy of atom interferometer phase measurement	$err = 10^{-4}$
Earth gravity field	$\vec{g} = \left\{0, 0, -9.8\mathrm{m/s}^2\right\}$
Proof mass	$W = 100\mathrm{kg}$
Proof mass density	$19250\mathrm{kg/m}^3$
The hole size	$L_n = 0.02\mathrm{m}$

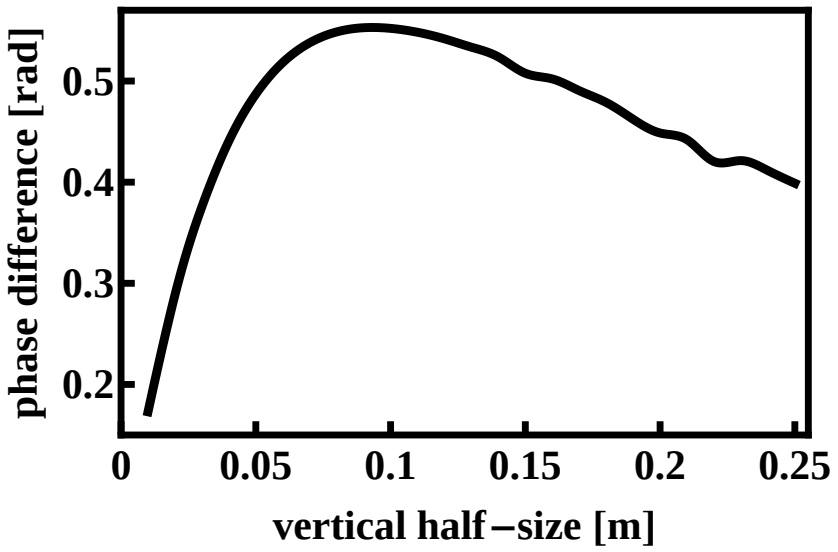

FIG. 2: Dependence of the maximum of phase difference on parallelepiped half-size

homogeneous density ρ and sizes $2a_x \times 2a_y \times 2a_z$ one has analytic expression [6, 8],

$$\begin{aligned}
\Phi &= -G\rho \sum_{j_x=-1}^{1} \sum_{j_y=-1}^{1} \sum_{j_z=-1}^{1} j_x j_y j_z f\left(x + j_x a_x, y + j_y a_y, z + j_z a_z\right), \\
f\left(u, v, w\right) &= -\frac{1}{2} w^2 \arctan\left(\frac{uv}{wr}\right) - \frac{1}{2} v^2 \arctan\left(\frac{uw}{vr}\right) - \frac{1}{2} u^2 \arctan\left(\frac{vw}{ur}\right) \\
&\quad + vw \ln\left(u + r\right) + uw \ln\left(v + r\right) + uv \ln\left(w + r\right), \\
r &= \sqrt{u^2 + v^2 + w^2}.
\end{aligned} \tag{5}$$

We performed calculations for Newtonian gravitational constant $G = 6.67428 * 10^{-11}\mathrm{m}^3\mathrm{s}^{-2}\mathrm{kg}^{-1}$. The proof mass shown in Fig. 1 consists of the parallelepipeds 1,2 and 3 for one half and 4,5 and 6 for another half.

Dependences of the maximal phase difference, position and velocity of maximum and minimum on the half-size of the proof mass $2L_z$ are shown in the Figs 2-4.

From the Fig. 2 one sees that the optimal phase difference has its own maximum. The value of this maximum and values of parameters we recommend to choose to observe it are presented in Table II.

II. ERROR MODEL

To achieve high precision of the interferometers' phase measurements one has to prepare with great accuracy both the atomic and proof mass system. In this section we determine requirements for preparation to achieve phase measurements with accuracy (4).

The most challenging here is precise positioning of the atom clouds [3]. The preferable here are, evidently, extrema of the clouds position. That is why found above extrema in $\{z, v\}$ space allow one not only maximize the response,

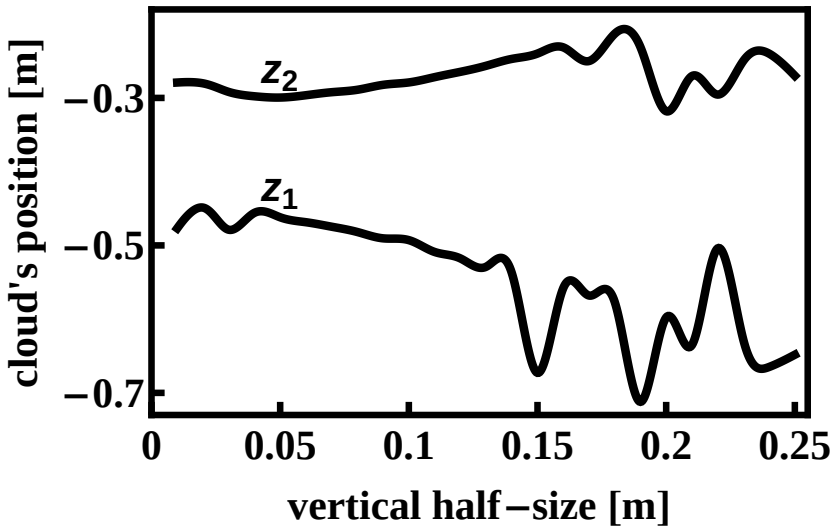

FIG. 3: Optimal position of the 1st and 2nd atom cloud

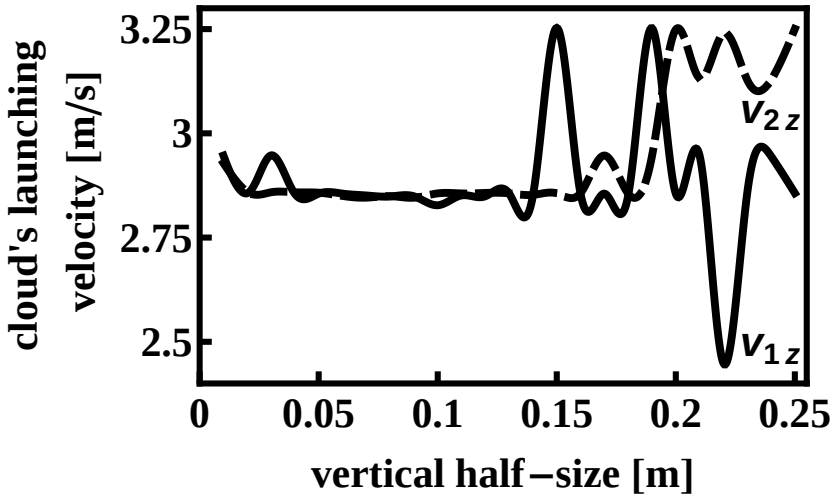

FIG. 4: Optimal launching velocities of the 1st and 2nd atom clouds

but also make less severe requirements for atom clouds position, velocity, temperature and size because the response becomes quadratic on variations of positions and velocities nea extrema.

Lets allow now small variations of the atom clouds initial positions, velocities and effective wave vector (atomic variables) and small displacement and rotation of proof mass halves (see Fig. 5). We expect that main contribution to response arises from joined proof mass halves, while for the separated halves contributions to the error decrease when the distance between halves increases. We determine below, in Sec. II A 2 a, the minimal distance L_d, starting from which the variations of contribution to the response from separated halves becomes smaller than ultimate phase error (4).

TABLE II: Optimal proof mass sizes and atom clouds positions and velocities to maximize the phase difference

phase difference	$\Delta\phi = 0.55271113$ rad
vertical half-size	$L_z = 0.09$m
horisontal half-size	$L_h = 0.08726$m
1st cloud position	$z_1 = -0.4904$m
1st cloud launching velocity	$v_{1z} = 2.849$m/s
2nd cloud position	$z_2 = -0.2823$m
2nd cloud launching velocity	$v_{2z} = 2.846$m/s

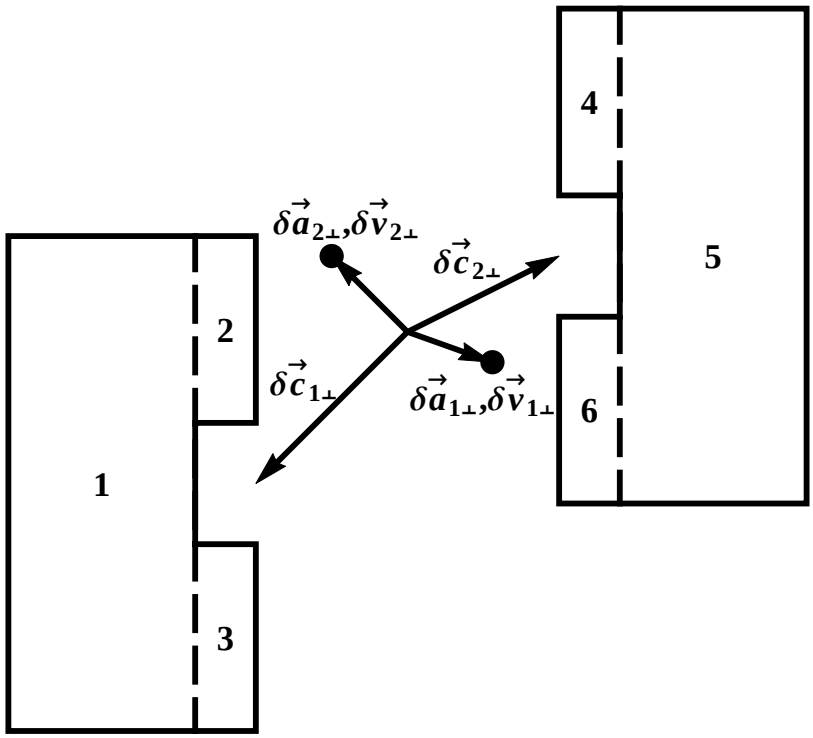

FIG. 5: Top view. Small variations of the atomic and proof mass variables. Variations of proof mass halves orientation and effective wave vector rotation are not shown.

A. Atomic variables

1. *Joined proof mass halves.*

For the given atom cloud (1 or 2 in Table II) lets denote as $\{\vec{a}_0, \vec{v}_0\}$ extremal position and velocity and $\vec{k}_0 = \{0, 0, k\}^T$ the vertical Raman field effective wave vector. Including variations one has to substitute in the Eq. (3)

$$\vec{a} = \vec{a}_0 + \delta\vec{a}, \tag{6a}$$
$$\vec{v} = \vec{v}_0 + \delta\vec{v}, \tag{6b}$$
$$\vec{k} = R_{\vec{k}}\vec{k}_0, \tag{6c}$$

where $\delta\vec{a}_i = \{\delta x_i, \delta y_i, \delta z_i\}^T$ for interferometer i. We assumed in (6c) that Raman field consists only from counter-propagating wave vectors, but laser axis could be slightly rotated from direction of $\vec{k}_0$. For the rotation matrix of this rotation we use Rodriguez rotation formula [9]

$$R_{\vec{k}ij} = \cos(\psi)\,\delta_{ij} + \frac{1-\cos(\psi)}{\psi^2}\psi_i\psi_j + \frac{\sin(\psi)}{\psi}\varepsilon_{ijm}\psi_m, \tag{7}$$

where $\vec{\psi}$ is an angle of rotation, δ_{ij} is Kronecker symbol, ε_{ijm} is absolutely antisymmetric tensor. For $\psi \ll 1$,

$$R_{\vec{k}ij} \approx \delta_{ij} + \varepsilon_{ijm}\psi_m - \frac{1}{2}\left(\psi^2\delta_{ij} - \psi_i\psi_j\right). \tag{8}$$

Using this expression and expanding in Eq. (3) up to the 2nd order in respect to $\delta\vec{a}, \delta\vec{v}$ and $\vec{\psi}$ one arrives to the following approximate expression for the phase

$$\begin{aligned}
\phi \approx\ & \vec{k}_0 \cdot (\tau_3\vec{u}_{30} - t_1\vec{u}_{20} + \vec{u}_{21} - \vec{u}_{31}) \\
& - \left(\vec{\psi} \times \vec{k}_0\right) \cdot (\tau_3\vec{u}_{30} - t_1\vec{u}_{20} + \vec{u}_{21} - \vec{u}_{31}) \\
& + \delta\vec{a}_p\vec{k}_{0i}\left(\tau_3 b_{pi30} - t_1 b_{pi20} + b_{pi21} - b_{pi31}\right) \\
& + \delta v_p\vec{k}_{0i}\left(\tau_3 b_{pi31} - t_1 b_{pi21} + b_{pi22} - b_{pi32}\right) \\
& + \frac{1}{2}\delta\vec{a}_p\delta\vec{a}_q\vec{k}_{0i}\left(\tau_3 d_{pqi30} - t_1 d_{pqi20} + d_{pqi21} - d_{pqi31}\right) \\
& + \frac{1}{2}\delta v_p\delta v_q\vec{k}_{0i}\left(\tau_3 d_{pqi32} - t_1 d_{pqi22} + d_{pqi23} - d_{pqi33}\right) \\
& + \frac{1}{2}\left[\vec{\psi} \times \left(\vec{\psi} \times \vec{k}_0\right)\right] \cdot (\tau_3\vec{u}_{30} - t_1\vec{u}_{20} + \vec{u}_{21} - \vec{u}_{31}) \\
& + \delta\vec{a}_p\delta\vec{v}_q\vec{k}_{0i}\left(\tau_3 d_{pqi31} - t_1 d_{pqi21} + d_{pqi22} - d_{pqi32}\right) \\
& - \delta\vec{a}_p\left(\vec{\psi} \times \vec{k}_0\right)_i\left(\tau_3 b_{pi30} - t_1 b_{pi20} + b_{pi21} - b_{pi31}\right) \\
& - \delta v_p\left(\vec{\psi} \times \vec{k}_0\right)_i\left(\tau_3 b_{pi31} - t_1 b_{pi21} + b_{pi22} - b_{pi32}\right),
\end{aligned} \tag{9a}$$

$$\vec{u}_{\alpha\beta} = \int_{\tau_{\alpha-1}}^{\tau_\alpha} dt t^\beta \delta\vec{g}\left(\vec{a}_0 + \vec{v}_0 t + \vec{g}\frac{t^2}{2}\right), \tag{9b}$$

$$b_{pi\alpha\beta} \equiv \int_{\tau_{\alpha-1}}^{\tau_\alpha} dt t^\beta \partial_p\delta\vec{g}_i\left(\vec{a}_0 + \vec{v}_0 t + \vec{g}\frac{t^2}{2}\right), \tag{9c}$$

$$d_{pqi\alpha\beta} = \int_{\tau_{\alpha-1}}^{\tau_\alpha} dt t^\beta \partial_p\partial_q\delta\vec{g}_i\left(\vec{a}_0 + \vec{v}_0 t + \vec{g}\frac{t^2}{2}\right). \tag{9d}$$

A summation convention is implicit in Eq. (9a) that will be used in all subsequent equations, in which repeated indices and symbols are to be summed over.

We calculated numerically coefficients in the expansion (9a) for the optimal conditions found in Sec. I. Different terms in the Eq. (9a) are presented in Table III. We changed sign of the terms associated with interferometer 2.

One sees that in spite of the using extremum points $\{z_i, v_i\}$ linear terms are not equal 0. It is because extrema $\{z_i, v_i\}$ have been found in Sec. I approximately. One can find that coefficients in the linear dependences so small that for allowed variations of position and velocity (see below Table IV) linear contributions are negligible.

One can use nonlinear terms to estimate atom clouds' radii and temperatures. Consider for example relative contribution

$$\delta\varphi_z = \alpha\delta z_i^2. \tag{10}$$

If Raman fields are sufficiently flat to neglect ac-Stark shift variation across the atom cloud and if Raman pulses are sufficiently short to neglect the Doppler broadening of the Raman transition, then one needs just to average (10) over atoms' spatial distribution. For Gaussian distribution, $\frac{\exp\left[-\delta z_i^2/\delta z_{i\max}^2\right]}{\sqrt{\pi}\delta z_{i\max}}$, after averaging one gets

$$\langle\delta\varphi_z\rangle = \frac{\alpha}{2}\delta z_{i\max}^2 \tag{11}$$

Requiring it to be equal expected relative error of phase measurement, *err*, one finds for atom cloud radius

$$\delta z_{i\max} = \sqrt{\frac{2 * err}{\alpha}}. \tag{12}$$

In the same manner we determine atom cloud velocities' variations, temperatures and angle of the wave vector rotation. These quantities are pieced together in the Table IV for relative error value 4

TABLE III: Error model for 100 kg proof mass

Term	relative weight
Linear in position	$-.03159\delta z_1$ $-0.05332\delta z_2$
Linear in velocity	$0.0005170\delta v_{1z}$ $-0.0001622\delta v_{2z}$
nonlinear in position	$46.32\left(\delta x_1^2+\delta y_1^2\right)$ $-92.64\delta z_1^2$ $17.89\left(\delta x_2^2+\delta y_2^2\right)$ $-35.79\delta z_2^2$
nonlinear in velocity	$3.981\left(\delta v_{1x}^2+\delta v_{1y}^2\right)$ $-7.962\delta v_{1z}^2$ $1.587\left(\delta v_{2x}^2+\delta v_{2y}^2\right)$ $-3.173\delta v_{2z}^2$
nonlinear in rotation	$-0.2782\left(\psi_{1x}^2+\psi_{1y}^2\right)$ $-0.2218\left(\psi_{2x}^2+\psi_{2y}^2\right)$
position-velocity cross term	$27.00\left(\delta v_{1x}\delta x_1+\delta v_{1y}\delta y_1\right)$ $-53.99\delta v_{1z}\delta z_1$ $10.42\left(\delta v_{2x}\delta x_2+\delta v_{2y}\delta y_2\right)$ $-20.83\delta v_{2z}\delta z_2$
position-rotation cross term	$-0.01580\left(\delta x_1\psi_{1y}-\delta y_1\psi_{1x}\right)$ $-0.02666\left(\delta x_2\psi_{2y}-\delta y_2\psi_{2x}\right)$
velocity-rotation cross term	$0.0002585\left(\delta v_{1x}\psi_{1y}-\delta v_{1y}\psi_{1x}\right)$ $-0.00008111\left(\delta v_{2x}\psi_{2y}-\delta v_{2y}\psi_{2x}\right)$

TABLE IV: Parameters of the atom interferometers one has to hold for proof mass 100 kg and relative error 10^{-4}.

1st cloud vertical radius $\delta z_{1\,\max}$ [m]	0.001469
1st cloud vertical velocity $\delta v_{1z\,\max}$ [m/s]	0.005012
1st cloud vertical temperature [K]	$2.070*10^{-7}$
1st cloud horizontal radius $\delta x_{1\,\max}$ [m]	0.002078
1st cloud horizontal velocity $\delta v_{1x\,\max}$[m/s]	0.007088
1st cloud horizontal temperature [K]	$4.139*10^{-7}$
1st interferometer wave vector rotation angle $\psi_{1\,\max}$ [rad]	0.02681
2nd cloud vertical radius $\delta z_{2\,\max}$ [m]	0.002364
2nd cloud vertical velocity $\delta v_{2z\,\max}$ [m/s]	0.007939
2nd cloud vertical temperature [K]	$5.193*10^{-7}$
2nd cloud horizontal radius $\delta x_{2\,\max}$ [m]	0.003343
2nd cloud horizontal velocity $\delta v_{2x\,\max}$ [m/s]	0.01123
2nd cloud horizontal temperature [K]	$1.039*10^{-6}$
2nd interferometer wave vector rotation angle $\psi_{2\,\max}$ [rad]	0.03003

2. *Separated proof mass halves.*

Contribution to the response from different terms in Eq. (9a) arising for separated proof mass halves are pieced together in the Table V.

The point here is that even if the contribution to the response from separated halves is small this case could be dangerous because launching positions and velocities found above become no more extrema of the phase, and therefore major contribution to the phase arises from the linear terms in Table V. The only way to decrease these linear error is to increase distance between proof masses L_d. Indeed for $L_d = 0.15$m linear in velocity errors can be 13 times large than ultimate relative accuracy (4). For $L_d = 0.3$m they are still 4 times larger. But for $L_d = 1$m all errors linear and nonlinear are well below than parameter *err*.

a. Minimal distance Since moving proof mass halves on the distances $\pm 1m$ could be a technological challenge, we determine here minimal half-distance L_d of proof mass halves separation. For quantitative consideration we accept here that the minimal L_d is a distance at which all relative errors in the 3rd columns of the Table V are smaller than parameter *err*. For example, for 100kg proof mass largest error in table V is linear in position of the second interferometer cloud δz_2. When effective wave vector is vertical, $\vec{k} = \{0, 0, k\}$, from Eq. (9a), one finds for this term

$$\varphi_d \equiv \left|k\left(\tau_3 b_{3330} - t_1 b_{3320} + b_{3321} - b_{3331}\right)\right| \delta z_{2\,\max}, \tag{13}$$

TABLE V: Contribution to response from separated proof mass halves. Phase decrease is a ratio of response to the phase difference for joined proof mass halves. We changed sign for terms related to interferometer 1. Three values in the curls correspond to the half-distance between proof masses L_d = 0.15m, 0.3m, and 1m respectively. Values of $\delta x_{i\,\max}$, $\delta z_{i\,\max}$, $\delta v_{ix\,\max}$, $\delta v_{iz\,\max}$, $\psi_{i\,\max}$ are taken from table IV.

Term	relative weight	$\delta x_i = \delta y_i = \delta x_{i\,\max}, \delta z_i = \delta z_{i\,\max}$, $\delta v_{ix} = \delta v_{iy} = \delta v_{ix\,\max}, \delta v_{iz} = \delta v_{iz\,\max}, \psi_i = \psi_{i\,\max}$
Phase decrease	$\{0.84669512, 0.95775894, 0.9979968\}$	
Linear in position	$\{0.3435, 0.1461, 0.009211\}\ \delta z_1$ $\{-0.5453, -0.1844, -0.009591\}\ \delta z_2$	$\{0.0005046762, 0.00021462856, 0.000013534148\}$ $\{-0.0012890354, -0.00043602961, -0.000022672662\}$
Linear in velocity	$\{0.09949, 0.04268, 0.002719\}\ \delta v_{1z}$ $\{-0.1619, -0.05464, -0.002839\}\ \delta v_{2z}$	$\{0.00049866914, 0.00021392743, 0.000013627868\}$ $\{-0.001285252, -0.00043379244, -0.000022539355\}$
nonlinear in position	$\{-5.532, -0.8019, -0.006320\}\ (\delta x_1^2 + \delta y_1^2)$ $\{3.751, 0.5657, 0.004688\}\ \delta z_1^2$ $\{-4.643, -0.6147, -0.004004\}\ (\delta x_2^2 + \delta y_2^2)$ $\{3.241, 0.4444, 0.002988\}\ \delta z_2^2$	$\{-4.777 * 10^{-5}, -6.924 * 10^{-6}, -5.458 * 10^{-8}\}$ $\{8.098 * 10\hat{}-6, 1.221 * 10\hat{}-6, 1.012 * 10\hat{}-8\}$ $\{-0.0001038, -0.00001374, -8.951 * 10\hat{}-8\}$ $\{0.00001811, 2.484 * 10\hat{}-6, 1.670 * 10\hat{}-8\}$
nonlinear in velocity	$\{-0.5135, -0.07803, -0.0006637\}\ (\delta v_{1x}^2 + \delta v_{1y}^2)$ $\{0.3424, 0.05444, 0.0004912\}\ \delta v_{1z}^2$ $\{-0.3943, -0.05179, -0.0003348\}\ (\delta v_{2x}^2 + \delta v_{2y}^2)$ $\{0.2758, 0.03748, 0.0002499\}\ \delta v_{2z}^2$	$\{-0.00005160, -7.840 * 10\hat{}-6, -6.669 * 10\hat{}-8\}$ $\{8.602 * 10\hat{}-6, 1.367 * 10\hat{}-6, 1.234 * 10\hat{}-8\}$ $\{-0.00009940, -0.00001306, -8.442 * 10\hat{}-8\}$ $\{0.00003477, 4.725 * 10\hat{}-6, 3.151 * 10\hat{}-8\}$
nonlinear in rotation	$\{0.04398, 0.01255, 0.0006208\}\ (\psi_{1x}^2 + \psi_{1y}^2)$ $\{0.03268, 0.008566, 0.0003808\}\ (\psi_{2x}^2 + \psi_{2y}^2)$	$\{0.00006323, 0.00001805, 8.926 * 10\hat{}-7\}$ $\{0.00005893, 0.00001544, 6.867 * 10\hat{}-7\}$
position-velocity cross term	$\{-3.245, -0.4732, -0.003779\}\ (\delta v_{1x}\delta x_1 + \delta v_{1y}\delta y_1)$ $\{2.196, 0.3332, 0.002802\}\ \delta v_{1z}\delta z_1$ $\{-2.686, -0.3551, -0.002309\}\ (\delta v_{2x}\delta x_2 + \delta v_{2y}\delta y_2)$ $\{1.876, 0.2568, 0.001724\}\ \delta v_{2z}\delta z_2$	$\{-0.00009559, -0.00001394, -1.113 * 10\hat{}-7\}$ $\{0.00001617, 2.454 * 10\hat{}-6, 2.063 * 10\hat{}-8\}$ $\{-0.0002017, -0.00002666, -1.734 * 10\hat{}-7\}$ $\{0.00003521, 4.819 * 10\hat{}-6, 3.235 * 10\hat{}-8\}$
position-rotation cross term	$\{1.114, 0.3560, 0.01893\}\ (\delta x_1\psi_{1y} - \delta y_1\psi_{1x})$ $\{-1.434, -0.4119, -0.01944\}\ (\delta x_2\psi_{2y} - \delta y_2\psi_{2x})$	0 0
velocity-rotation cross term	$\{0.3259, 0.1045, 0.005593\}\ (\delta v_{1x}\psi_{1y} - \delta v_{1y}\psi_{1x})$ $\{-0.4251, -0.1220, -0.005755\}\ (\delta v_{2x}\psi_{2y} - \delta v_{2y}\psi_{2x})$	0 0

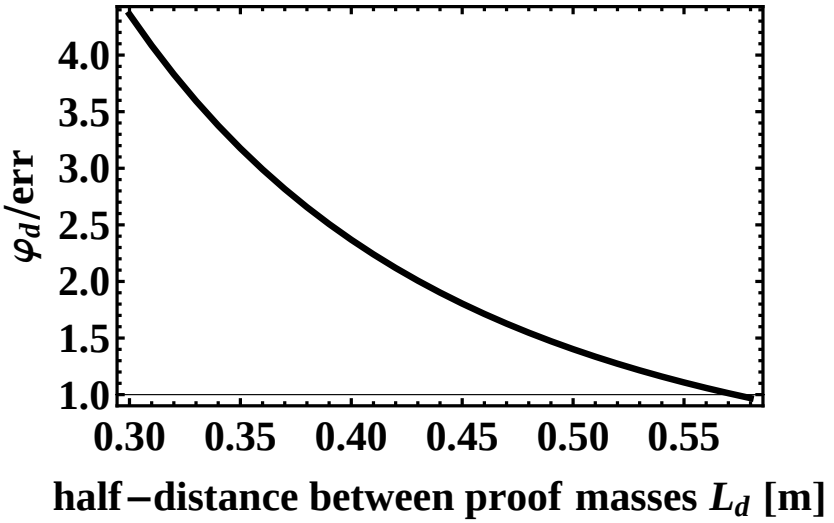

FIG. 6: Dependence of the error (13) on the half-distance between proof mass halves L_d.

where tensor b is defined in Eq. (9c) and maximal variation of the atom cloud vertical position, $\delta z_{2\,\max}$, one finds in the table IV. Fig. 6 shows dependence of the term (13) on the half distance L_d.

One sees that φ_d becomes smaller than err at $L_d = 0.58m$. From the error model for this half-distance , presented at the table VI , one sees that all other errors are also smaller than err.

TABLE VI: The same as in the Table V, but for the distance between proof mass halves $L_d = 0.58$m.

Term	relative weight	$\delta x_i = \delta y_i = \delta x_{i\,\max}, \delta z_i = \delta z_{i\,\max}$, $\delta v_{xi} = \delta v_{yi} = \delta v_{xi\,\max}, \delta v_{zi} = \delta v_{zi\,\max}, \psi_i = \psi_{i\,\max}$
Phase decrease	0.99128250	
Linear in position	$0.03715\delta z_1$	0.00005459
	$-0.04099\delta z_2$	-0.00009691
Linear in velocity	$0.01093\delta v_{1z}$	0.00005477
	$-0.01214\delta v_{2z}$	-0.00009635
nonlinear in position	$-0.06795\left(\delta x_1^2 + \delta y_1^2\right)$	$-0.5868 * 10^{-6}$
	$0.04963\delta z_1^2$	$0.1071 * 10^{-6}$
	$-0.04620\left(\delta x_2^2 + \delta y_2^2\right)$	$-0.1033 * 10^{-5}$
	$0.03420\ \delta z_2^2$	$0.1911 * 10^{-6}$
nonlinear in velocity	$-0.006947\left(\delta v_{1x}^2 + \delta v_{1y}^2\right)$	$-0.6980 * 10^{-6}$
	$0.005046\delta v_{1z}^2$	$0.1268 * 10^{-6}$
	$-0.003872\left(\delta v_{2x}^2 + \delta v_{2y}^2\right)$	$-0.9761 * 10^{-6}$
	$0.002867\ \delta v_{2z}^2$	$0.1807 * 10^{-6}$
nonlinear in rotation	$0.002667\left(\psi_{1x}^2 + \psi_{1y}^2\right)$	$0.3835 * 10^{-5}$
	$0.001692\left(\psi_{2x}^2 + \psi_{2y}^2\right)$	$0.3051 * 10^{-5}$
position-velocity cross term	$-0.04042\left(\delta v_{1x}\delta x_1 + \delta v_{1y}\delta y_1\right)$	$-0.1191 * 10^{-5}$
	$0.02949\delta v_{1z}\delta z_1$	$0.2172 * 10^{-6}$
	$-0.02666\left(\delta v_{2x}\delta x_2 + \delta v_{2y}\delta y_2\right)$	$-0.2001 * 10^{-5}$
	$0.01974\delta v_{2z}\delta z_2$	$0.3704 * 10^{-6}$
position-rotation cross term	$0.07976\left(\delta x_1\psi_{1y} - \delta y_1\psi_{1x}\right)$	0
	$-0.08506\left(\delta x_2\psi_{2y} - \delta y_2\psi_{2x}\right)$	0
velocity-rotation cross term	$0.02351\left(\delta v_{1x}\psi_{1y} - \delta v_{1y}\psi_{1x}\right)$	0
	$-0.02518\left(\delta v_{2x}\psi_{2y} - \delta v_{2y}\psi_{2x}\right)$	0

B. Proof mass variables

In this section we consider errors arising from variations of the joined proof mass halves position and orientation. When the proof mass frame shifted on $\delta\vec{c}$ and rotated on angle $\vec{\psi}$ in respect to the lab. frame Eqs. (3) have to be rewritten as

$$\phi = \vec{k}' \cdot \left(\tau_3\vec{u}_{30} - t_1\vec{u}_{20} + \vec{u}_{21} - \vec{u}_{31}\right), \tag{14a}$$

$$\vec{u}_{\alpha\beta} = \int_{\tau_{\alpha-1}}^{\tau_\alpha} dt t^\beta \delta\vec{g}\left(\vec{a}' + \vec{v}'t + \vec{g}'_E\frac{t^2}{2}\right), \tag{14b}$$

where

$$\vec{k}' = R\vec{k}_0, \tag{15a}$$

$$\vec{a}' = R\left(\vec{a}_0 - \delta\vec{c}\right), \tag{15b}$$

$$\vec{v}' = R\vec{v}_0, \tag{15c}$$

$$\vec{g}'_E = R\vec{g}_E \tag{15d}$$

are, respectively, wave vector, atoms' launching position, atoms launching velocity, and Earth gravity field in the proof mass frame, R is rotation matrix. Configurations considered above could not be optimal for both halves of the proof mass and we allow the variations of these halves to be independent then linear in $\delta\vec{c}$ and $\vec{\psi}$ terms should dominate. So in this section we consider only linear corrections to the phase, when

$$R_{ij} \approx \delta_{ij} + \varepsilon_{ijm}\psi_m. \tag{16}$$

Expanding in Eq. (14b) to the linear terms brings one to the following expression for the phase

$$\begin{aligned}\phi \approx & \vec{k}_0 \left(\tau_3 \vec{u}_{30} - t_1 \vec{u}_{20} + \vec{u}_{21} - \vec{u}_{31}\right) \\ & - \left(\vec{\psi} \times \vec{k}_0\right) \left(\tau_3 \vec{u}_{30} - t_1 \vec{u}_{20} + \vec{u}_{21} - \vec{u}_{31}\right) \\ & - \left(\delta\vec{c} + \vec{\psi} \times \vec{a}_0\right)_p \vec{k}_i \left(\tau_3 b_{pi30} - t_1 b_{pi20} + b_{pi21} - b_{pi31}\right) \\ & - \left(\vec{\psi} \times \vec{v}_0\right)_p \vec{k}_i \left(\tau_3 b_{pi31} - t_1 b_{pi21} + b_{pi22} - b_{pi32}\right) \\ & - \frac{1}{2} \left(\vec{\psi} \times \vec{g}_E\right)_p \vec{k}_i \left(\tau_3 b_{pi32} - t_1 b_{pi22} + b_{pi23} - b_{pi33}\right), \end{aligned} \tag{17}$$

where tensor $b_{pi\alpha\beta}$ is defined in Eq. (9c). For the chosen proof mas halves' geometry, location and orientation and unperturbed atomic variables, numeric integration brings one to the following linear dependence of the phase difference

$$\Delta\phi \approx 0.5527 \left[1 + 6.782 \left(\delta c_{1x} - \delta c_{2x}\right) + 0.04246 \left(\delta c_{1z} + \delta c_{2z}\right) - 0.09261 \left(\psi_{1y} - \psi_{2y}\right)\right] \tag{18}$$

where variation of the left (right) half-proof mass position and angle of rotation are $\delta\vec{c}_1$ $(\delta\vec{c}_2)$ and $\vec{\psi}_1$ $\left(\vec{\psi}_2\right)$. One sees that the phase is most sensitive to displacement along $x-$axis (see Fig. 1a). From the symmetric shapes there are no linear sensitivity to the displacement along $y-$axis, rotations in respect to the $z-$ and $x-$axes. When one synchronize displacement along $x-$axis and rotation of both proof mass halves corresponding linear dependences disappear. Since in the absence of rotation synchronized displacement of the proof mass halves is equivalent to the synchronized displacement of both interferometers in the opposite directions, the slopes of the linear dependences on δz_i equal to the average slopes in the linear dependences on the interferometers' displacement taken with opposite sign [compare corresponding coefficients in Eq. (18) and first 2 rows in the Tables III]. Since for optimal configuration $z-$coordinates of the atom clouds launching points are closed to the extrema, the slopes of the dependence on δc_{iz} in Eq. (18) are 2 orders of magnitude smaller than slopes of the dependence on δc_{ix}.

From the Eq. (18) one concludes that ultimate accuracy (4) can be achieved for proof mass halves positioning with accuracy

$$\left|\delta c_{ix}\right| < 14.74\mu, \tag{19a}$$

$$\left|\psi_{iy}\right| < 1.08\text{mrad}. \tag{19b}$$

III. CONCLUSION

We showed that 100kg Tungsten proof mass can produce change in the atom interferometers phase double difference

$$\delta\Delta\phi = 0.54789287\text{rad} \tag{20}$$

for the ^{133}Cs atom interferometers, with parameters listed in Table I, extremal values of atom interferometers launching position and velocities and proof mass sizes listed in Table II. The response (20) is comparable with that observed in [3], but the choice of phase's extrema allowed us to make requirements for atoms' positioning 2 orders of magnitude less severe than requirements for proof mass halves positioning [compare (19a) and data in Table IV].

Acknowledgments

Author is appreciated to Drs. M. Kasevich, B. Young, S. Libby, M. Matthews, T. Loftus, M. Shverdin, V. Sonnad and A. Zorn for fruitful discussion and collaboration. Special gratefulness to S. Libby and V. Sonnad who showed me their unpublished results, and to Dr. A. Zorn, who brought to my attention article [8].

The support of this work by Lawrence Livermore National Laboratory, LDRD 12- LW-009: "High-Precision Test of the Gravitational Inverse-Square Law with an Atom Interferometer,"is gratefully acknowledged. This work was partially performed under the auspices of the U.S. Department of Energy by Lawrence Livermore National Laboratory under Contract DE-AC52-07NA27344.

[1] B. Dubetsky, A. P. Kazantsev, V. P. Chebotayev, V. P. Yakovlev, Pis'ma Zh. Eksp. Teor. Fiz. 39, 531 (1984) [JETP Lett. 39, 649 (1984)].

[2] Fixler, J. B., Foster, G. T., McGuirk, J. M. & M. A. Kasevich, Science 315, 74 (2007).
[3] G. Rosi, F. Sorrentino, L. Cacciapuoti, M. Prevedelli & G. M. Tino, Nature **510**, 518 (2014).
[4] M. J. Snadden, J. M. McGuirk, P. Bouyer, K. G. Haritos, and M. A. Kasevich, Phys. Rev. Lett. 81, 971 (1998).
[5] M. Kasevich, S. Chu, Phys. Rev. Lett., 67, 181 (1991).
[6] B. Dubetsky, Private communications, 2008
[7] http://periodictable.com/Properties/A/Density.al.html
[8] Z. F. Seidov, P. I. Skvirsky, arXiv:astro-ph/0002496v1
[9] J. W. Gibbs, E. B. Wilson, "Vector analysis," New York : Charles Scriber's Sons London: Edward Arnold 1901, p. 338.